ResearchGate

See discussions, stats, and author profiles for this publication at: https://www.researchgate.net/publication/245434544

Bare wire anodes for electrodynamic tethers

Article *in* Journal of Propulsion and Power · May 1993

DOI: 10.2514/3.23629

CITATIONS
173

READS
202

3 authors, including:

Manuel Martinez-Sanchez
Massachusetts Institute of Technology
294 PUBLICATIONS **3,187** CITATIONS

SEE PROFILE

Eduardo Ahedo
University Carlos III de Madrid
193 PUBLICATIONS **2,139** CITATIONS

SEE PROFILE

Some of the authors of this publication are also working on these related projects:

LEOSWEEP View project

ESA MODEX View project

All content following this page was uploaded by Manuel Martinez-Sanchez on 25 March 2015.

The user has requested enhancement of the downloaded file.

JOURNAL OF PROPULSION AND POWER
Vol. 9, No. 3, May–June 1993

Bare Wire Anodes for Electrodynamic Tethers

J. R. Sanmartín*
Universidad Politécnica de Madrid, Madrid 28040, Spain
and
M. Martínez-Sánchez† and E. Ahedo‡
Massachusetts Institute of Technology, Cambridge, Massachusetts 02139

The collection of electrons from the ionosphere is the major problem facing high-power electrodynamic tethers. This article discusses a simple electron-collection concept which is free of most of the physical uncertainties associated with plasma contactors in the rarefied, magnetized environment of an orbiting tether. The idea is to leave exposed a fraction of the tether length near its anodic end, such that, when a positive bias develops locally with respect to the ambient plasma, and for a tether radius small compared with both thermal gyroradius and Debye length, electrons are collected in an orbital-motion-limited regime. It is shown that large currents can be drawn in this way with only moderate voltage drops. The concept is illustrated through a discussion of performance characteristics for generators and thrusters.

Nomenclature

$A_{\rm eff}$ = effective collecting area
A_t = tether cross section
B = geomagnetic field
d = tether diameter
$\mathscr{E}$ = supplied electromotive force
E_m = motional electric field along tether direction
e = elementary charge
f = thrust
I = current along the tether
i = dimensionless current
J = current density
k_B = Boltzmann constant
L = tether length
L_B = length of segment AB
l_e = electron thermal gyroradius
M = tether mass
$m_{e,i}$ = electron (ion) mass
n = plasma density
R = load impedance
r_A = spherical anode radius
T = temperature
V = potential
$v_{\rm orb}$ = orbital velocity
W_g = load power in generator mode
W_m = mechanical power
w = dimensionless useful power
w_M = dimensionless optimum power for fully bare tether
x = ratio $\Delta V_A/\Delta V_B$ in the thruster mode
y = spatial coordinate along the tether
ΔV = potential bias, $V_t - V_p$
ϵ = $(m_e/m_i)^{1/2}$
ε = surface emissivity
ε_0 = free space permittivity
η = efficiency
λ_D = Debye length
ξ = y/L_*
ρ = tether mass density
σ = tether conductivity
σ_B = Stephan-Boltzmann constant
φ, ψ = dimensionless potential bias, $\psi = -\varphi$

Subscripts
A = anode or anodic end
B = point B
bk = background
C = cathode or cathodic end
p = plasma
t = tether
∞ = unperturbed plasma conditions
$*$ = characteristic value

Superscript
s = equivalent standard tether

Received March 25, 1991; revision received Feb. 17, 1992; accepted for publication Aug. 25, 1992. Copyright © 1993 by the American Institute of Aeronautics and Astronautics, Inc. All rights reserved.

*Professor of Physics, Escuela Técnica Superior de Ingenieros Aeronáuticos, Ciudad Universitaria.
†Associate Professor, Department of Aeronautics and Astronautics, Room 37-401. Member AIAA.
‡Assistant Professor; currently at Escuela Técnica Superior de Ingenieros Aeronáuticos, Ciudad Universitaria.

I. Introduction

ELECTRODYNAMIC tethers appear as promising devices for both high-power probing of the ionosphere and technical applications. Effective and reliable anodic contactors remain the principal difficulty facing such tethers,[1] although the ongoing theoretical and experimental work on plasma contactor physics may lead to a viable technology. In the interim, and also in any case as a long-term alternative, other contactor implementations are still necessary.

The generic problem is the need for a very large collecting area, since the ambient electron density is so low that the random current density may be of the order of 1 mA/m^2. Although the voltage bias of a typical anode strives to enlarge the "contact" area, Debye-sheath shielding makes this ineffective. An additional obstacle is the channeling of electrons by the geomagnetic field, which restricts collection to essentially one dimension. Plasma contactors[2,3] might overcome these problems by 1) emitting ions to provide quasineutrality, and 2) scattering electrons away from their guiding magnetic lines. The open mesh concept[1] uses the enlarged capture area of wire mesh to present a large apparent area with a small mass and neutral gas blockage.

In this article we present a concept which exploits the effectiveness of a thin cylinder as an electron collector, and further simplifies implementation by using the tether itself for

the purpose. Section II explains the physical basis of the device and gives some estimates of performance for current generation and thrust. A more rigorous analysis of a tether generator based on a bare-wire anode is given in Sec. III, and the application to a tether thruster is analyzed in Sec. IV. Section V summarizes the results.

II. Principle of Operation and Performance Potential

Consider the standard tether: a straight, metallic, insulated cable in a low-latitude orbit. In a reference frame tied to the tether, the ionospheric plasma is subject to the motional electric field $-\underset{\sim}{v}_{\text{orb}} \times B$, its projection E_m along the cable generating a current I_C across any interposed useful load. This current, which will be some fraction i_C of its short circuit value

$$I_C = i_C J_* A_t, \qquad J_* \equiv \sigma E_m$$

must be drawn by the anode from the ionosphere. From this point of view it can always be written as the product of the electron random current density, $J_\infty = \frac{1}{4} e n_\infty (8 k_B T_\infty / \pi m_e)^{1/2}$, and an appropriate "effective" area for the anode A_{eff}

$$I_C = J_\infty A_{\text{eff}}$$

Equating both expressions one has

$$A_{\text{eff}}/A_t = i_C J_*/J_\infty \tag{1}$$

Characteristic values for field, $E_m = 200$ V/km, conductivity, $\sigma = 3.5 \times 10^7\ \Omega^{-1}\,\text{m}^{-1}$ (aluminum), and plasma temperature, $k_B T_\infty = 0.1$ eV, give $A_{\text{eff}}/A_t = 8 i_C \times 10^9$ at $n_\infty = 10^{11}\ \text{m}^{-3}$, and $J_* = 7$ A/mm^2. For efficient generation i_C should clearly be moderately small (typically, $i_C \sim 0.1$–0.2, as later shown). A current $I_C \sim 10$ A would thus require a cable cross section $A_t \sim 10$ mm^2, and the anodic effective area would be extremely large ($\sim 10^4$ m^2).

Certainly, since the anode may sustain some voltage drop ΔV_A, it will exhibit some area gain, i.e., the actual area of its collecting surface need not be as large as A_{eff}. The Debye length, $\lambda_D \equiv (\varepsilon_0 k_B T_\infty / e^2 n_\infty)^{1/2}$, is small, however; for $k_B T_\infty = 0.1$ eV and $n_\infty = 10^{11}\ \text{m}^{-3}$ we have $\lambda_D \simeq 7.4$ mm. Thus, a typical passive anode is effectively shielded by space-charge; it takes too large a potential ΔV_A to produce a thick sheath or large gain. For instance, in the case of a sphere of radius $r_A \gg \lambda_D$, well-known results from probe theory for an unmagnetized plasma with equal temperatures give[4]

$$\frac{e\Delta V_A}{k_B T_\infty} \simeq \left(\frac{A_{\text{eff}}}{4\pi\lambda_D^2}\right)^{2/3} \frac{F(r_{\text{eff}}/r_A)}{(4\pi)^{1/3}} \tag{2}$$

where $r_{\text{eff}}^2 \equiv A_{\text{eff}}/4\pi$, F is a function given by Lam, and here $A_{\text{eff}}/4\pi\lambda_D^2 \simeq 1.7 \times 10^6 \times A_t\ (\text{mm}^2)$. To be definite, consider an area gain $A_{\text{eff}}/4\pi r_A^2 = 50$, giving $A_{\text{eff}} > 5000$ m^2 for $r_A = 3$ m. We then have $r_{\text{eff}} \simeq 7 r_A$ and $F \simeq 10$, and obtain an extremely high voltage drop $\Delta V_A \simeq 6125\ \text{V} \times [A_t\ (\text{mm}^2)]^{2/3}$. Although a future contactor, an active anode that emits ions (and electrons) might be effective against shielding,[5] it would yet have to face the strong magnetic guiding of electrons from the effective to the anodic surface. This is because l_e for $B \sim 0.3 \times 10^{-4}$ T, is also small; at the particular speed $(\pi k_B T_\infty / 2 m_e)^{1/2}$ we have $l_e \simeq 30$ mm.

Our bare-tether generator is based on a two-fold concept that avoids both λ_D and l_e effects. First, we claim that a good passive anode for the conditions of interest should have two (disparate) characteristic lengths, instead of just one as in the case of a sphere. The simplest example would be a cylinder of length much greater than its radius. Clearly, electron collection would be governed by the stronger gradients, and therefore, would be a two-dimensional process. If the radius is small enough, there is neither space-charge nor magnetic-guiding effects; the current is orbital-motion-limited (OML) and takes the largest possible value for given geometry and potential bias. If, in addition, the cylinder is long enough, the anodic area could take any desired value, e.g., 10^2 m^2.

A collecting area of 10^2 m^2 can be obtained with a length under 10 km if the radius is 2 mm or over. Note that the radius-to-Debye length ratio is then not very small. Fortunately, for cylindrical geometry, and in the absence of a magnetic field, the OML regime covers the entire range for this ratio, from zero to values of order unity (in three-dimensional geometry, and because the electric field is then steeper, the OML regime is attained, on the contrary, only in the limit $r_A/\lambda_D \to 0$).[6] Again, because of the two-dimensional geometry, we do expect here negligible magnetic effects. Although the current in the presence of a field B is not generally known, there exists a ("canonical") upper-bound to the current.[7] For a sphere, and even if r_A/l_e is small, the OML current exceeds that bound when $e\Delta V_A/k_B T_e$ is large enough—the condition of interest for the tether. The opposite holds, however, in the case of a cylinder. Since its radius would be here aound $0.1 l_e$, magnetic forces might indeed be dropped against electric forces.

Secondly, we can actually do away with the cylinder, because the tether itself, if uninsulated, may serve as anode. There are potential differences between points in the wire and the surrounding plasma; electrons will be collected by those bare segments that are biased positive to the local plasma. For a normal W-E orbit, the promising configuration for a generator is shown in Fig. 1, with the cable deployed upwards. The slope of the plasma potential line V_p arises from the motional field, while that of the tether potential line V_t is due to the ohmic loss. The local bias, $\Delta V \equiv V_t - V_p$, takes some peak value $\Delta V_A > 0$ at the anodic end, and remains positive over a segment AB (Fig. 1). This segment, if directly exposed to the plasma, will collect electrons as an OML cylindrical probe. For $e\Delta V \gg k_B T_\infty$, the OML current per unit length is given by[8]

$$\frac{dI}{dy} = e n_\infty d (2e\Delta V/m_e)^{1/2} \tag{3}$$

where d is the diameter $(4A_t/\pi)^{1/2}$. Electrons are ejected at the cathodic end C by some device such as a thermionic emit-

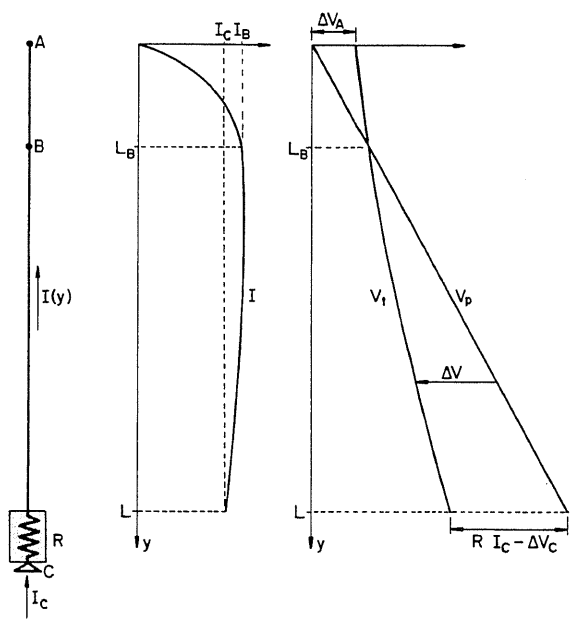

Fig. 1 Upward-deployed (partially or fully) bare tether operating in the generator mode. The segment AB, where $\Delta V = V_t - V_p > 0$, acts as an electron-collecting anode, while the segment BC is negatively biased, $\Delta V < 0$, and, if bare, collects ions. RI_C is the load voltage drop. A cathodic device placed at the bottom end C ejects an electron current I_C at a cost $\Delta V_C < 0$, here neglected.

ter, or a hollow cathode, at a cost of a (negative) voltage drop ΔV_C.

The anodic current $J_\infty A_{\text{eff}}$ may now be written as the average dI/dy times L_B. At small i_C we have $d\Delta V/dy \simeq$ const and the average is $\frac{2}{3}$ of the peak value; thus, we find

$$A_{\text{eff}} \simeq \pi d L_B \tfrac{2}{3}(4e\Delta V_A/\pi k_B T_\infty)^{1/2} \tag{4}$$

For an area gain $A_{\text{eff}}/\pi d L_B = 50$ one obtains $\Delta V_a \simeq 442$ V, a reasonable potential. For i_C small we also have ΔV_A nearly equal to $E_m L_B$. Ignoring collection in the remainder of the tether (segment BC), we may use Eqs. (1) and (4) to write

$$\Delta V_A/E_m \simeq L_B \simeq (2i_C)^{2/3} L_* \tag{5}$$

where the length

$$L_* \equiv (9\pi m_e \sigma^2 E_m A_t/128 e^3 n_\infty^2)^{1/3} \tag{6}$$

was introduced for later convenience. For $E_m = 200$ V/km and aluminum

$$L_* \text{ (km)} \simeq 10.6[A_t \text{ (mm}^2)]^{1/3}(10^{11} \text{ m}^{-3}/n_\infty)^{2/3}$$

Note that an oxidation-resistant conducting coating might be needed to avoid an oxyde layer caused by atomic oxygen if an Al tether is used.

Ion current into the segment BC could be suppressed by insulating this segment. A secondary problem with standard tethers is that insulating high voltages may place a bound on the tether length and, indirectly, on the power generated. A similar bound might exist for our partially bare tether. An interesting variant of our concept would be to let the wire go fully bare, doing away with insulation problems. Ion collection into BC follows the same law [Eq. (3)], using m_i instead of m_e, as long as $e|\Delta V|$ is large compared with both $k_B T_\infty$ and $\frac{1}{2} m_i v_{\text{orb}}^2$ (~10 eV). For O^+ ions, the current per unit length, at a given bias, would be smaller than the corresponding value for electrons by a factor $(m_e/m_i)^{1/2} \simeq \frac{1}{172}$. The bias, however, is roughly proportional to the length so that the current varies as (length)$^{3/2}$. Thus, there should be some upper bound to the efficiency: a ratio L_B/L, if too low, would produce a large ionic current; if too high, would reduce the voltage available at the load. Surface effects due to ion impacts on BC are discussed in the next section.

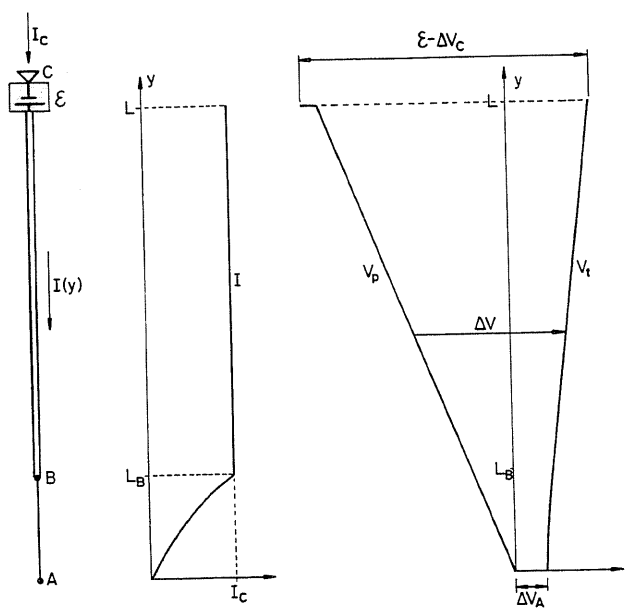

Fig. 2 Downward-deployed partially bare tether operating in the thruster mode. The segment AB is bare and operates as an electron-collecting anode; the segment BC is insulated. The potential bias ΔV is positive along the entire tether.

For a bare thruster, the promising configuration is that of a downward-deployed tether (Fig. 2). Its full length will be electron collecting unless sections of it are insulated. Because of this, a fully bare cable in the thruster mode will, on the one hand, have a much higher current-collection capability than a similarly sized generator tether, but on the other hand, will also have a lower efficiency, as the electrons collected near the emitting cathode at the top will do very little push work, but will still be accelerated through the cathodic voltage drop. For most applications, then, it will be advantageous to insulate the larger portion of the cable, leaving only a fixed section AB at the bottom intentionally exposed.

A detailed analysis of the above concepts, allowing for the spatial distribution of current and voltage bias, is presented in the next two sections. We obtain simple analytical results and complete dimensionless performance charts. We also make a detailed comparison to the standard tether. We shall consider in our analysis that the tether works in a limited density range (either by day, $n_\infty \sim 10^{12}$ m^{-3}, or by night, $n_\infty \sim 10^{11}$ m^{-3}).

III. Generator Mode

A. Standard Tether

The circuit equation for a standard tether is

$$E_m L = (R + L/\sigma A_t) I_C + \Delta V_A \tag{7}$$

where $\Delta V_A(I_C)$ is the unknown anode characteristic, which will depend on a number of parameters (n_∞, T_∞, B, anodic geometry . . .). In Eq. (7) we neglected the ionospheric closure impedance due to both Alfven and whistler band radiation; applying the algorithm of Ref. 9 to our case, it has been estimated to be typically less than 1 Ω. We also neglected the cathode potential drop ΔV_C, which, for the same current, should be much less than ΔV_A.[1] Given the characteristic $\Delta V_A(I_C)$ and both E_m and J_* (or σ), Eq. (7) determines I_C for selected values of three free parameters: A_t, L, and R. The mechanical power extracted from the orbital motion W_m, the generated power W_g, and the mass M of the conducting wire of density ρ are determined by simple expressions

$$W_m = E_m L I_C \tag{8}$$

$$W_g = R I_C^2, \qquad M = \rho A_t L \tag{9}$$

We also introduce the generator efficiency, $\eta \equiv W_g/W_m$, and a (dimensionless) useful power per unit mass of wire, $w \equiv \rho W_g/E_m J_* M$.

We may now consider A_t, L, and *one* among the dimensionless quantities η, w, and i_C, as our free parameters. The *two* other dimensionless quantities could then be obtained from equations

$$\eta = 1 - i_C - \Delta V_A(i_C J_* A_t)/E_m L \tag{10}$$

$$w = i_C \eta \tag{11}$$

which follow from Eqs. (7–9). Finally, useful power, power per unit mass, load impedance, and current, would be directly determined by the expressions

$$W_g = J_* E_m A_t L w, \qquad W_g/M = J_* E_m w/\rho \tag{12}$$

$$R = E_m L w/J_* A_t i_C^2, \qquad I_C = J_* A_t i_C \tag{13}$$

For aluminum ($\rho \simeq 2.7 \times 10^3$ kg/m^3) and $E_m = 200$ V/km, we have (in addition to $J_* \simeq 7$ A/mm^2) $J_* E_m \simeq 1.4$ kW/km

$\times$ mm^2, $J_*E_m/\rho \simeq 0.52$ kW/kg and $E_m/J_* \simeq 28.6\ \Omega \times$ mm^2/km. Note that, according to Eq. (12), the power per unit mass fixes w, and then W_g determines the volume A_tL.

For ΔV_A negligible (ideal tether), Eqs. (10) and (11) read

$$\eta = 1 - i_C, \qquad w = i_C(1 - i_C)$$

and describe the well-known power-efficiency tradeoff common to most electrical generators. Although w is maximum at $i_C = \eta = 0.5$, reducing i_C to improve the efficiency has little effect at first on w. However, the trend reverses at lower i_C. Thus, in a sense, best values for i_C, $1 - \eta$, and w are centered at 0.25 or 0.2.

Equations (10) and (11) for the real tether modify this result. Both ΔV_A and $\mathrm{d}\Delta V_A/\mathrm{d}I_C$ will be positive; thus, the maximum of $w(i_C)$, at given A_t and L, occurs at certain $i_C < 0.5$. For a tether not far from ideal, the best i_C-range will be centered at, i.e., 0.15 or 0.2. Note, further, that for given w and A_tL (or W_g and W_g/M), the efficiency grows with growing L (or decreasing A_t) because both E_mL increases and ΔV_A decreases (again, $\mathrm{d}\Delta V_A/\mathrm{d}I_C > 0$).

B. Partially Bare Tether

Equations (7) and (8) take new forms for a bare tether. If segment BC is insulated, the circuit equation may be written from Fig. 1 as

$$E_mL = \{R + [(L - L_B)/\sigma A_t]\}I_C + E_mL_B \qquad (14)$$

To find W_m, note that the faraway plasma potential is given by $\mathrm{d}V_p/\mathrm{d}y = E_m$, while current and potential inside the tether satisfy Ohm's law, $I(y) = \sigma A_t \mathrm{d}V_t/\mathrm{d}y$. The equation for the local bias voltage is

$$\frac{\mathrm{d}\Delta V}{\mathrm{d}y} = \frac{I}{\sigma A_t} - E_m \qquad (15)$$

Using $\Delta V_B = 0$ and $W_m = \int_0^L E_m I(y)\,\mathrm{d}y$, we find

$$W_m = E_m(L - L_B)I_C + J_*A_t(E_mL_B - \Delta V_A) \qquad (16)$$

Expressions for both L_B and ΔV_A are now required.

Introducing dimensionless variables $\xi \equiv y/L_*$, $\varphi = \Delta V(y)/E_mL_*$, and $i = I(y)/J_*A_t$, Eqs. (3) and (15) become

$$\frac{\mathrm{d}i}{\mathrm{d}\xi} = \frac{3}{4}\varphi^{1/2} \qquad (17)$$

$$\frac{\mathrm{d}\varphi}{\mathrm{d}\xi} = i - 1 \qquad (18)$$

An immediate first integral is $i^2 - 2i - \varphi^{3/2} = \text{const}$. Using boundary conditions $\varphi = \varphi_A$, $i = 0$ and $\varphi = 0$, $i = i_C$, yields

$$\varphi_A = (2i_C - i_C^2)^{2/3} \qquad (19)$$

Also, taking i from Eq. (18) gives a relation between $\mathrm{d}\varphi/\mathrm{d}\xi$ and φ. With boundary conditions $\varphi = \varphi_A$ at $\xi = 0$ and $\varphi = 0$ at $\xi = \xi_B$, we obtain the potential profile $\varphi(\xi)$, and in particular

$$\xi_B = \int_0^{\varphi_A} \mathrm{d}\varphi[1 - \varphi_A^{3/2} + \varphi^{3/2}]^{-1/2} \qquad (20)$$

at small i_C we find $\xi_B \simeq (2i_C)^{2/3}$, recovering Eq. (5). We finally have

$$\Delta V_A = E_mL_*\varphi_A(i_C), \qquad L_B = L_*\xi_B(i_C) \qquad (21)$$

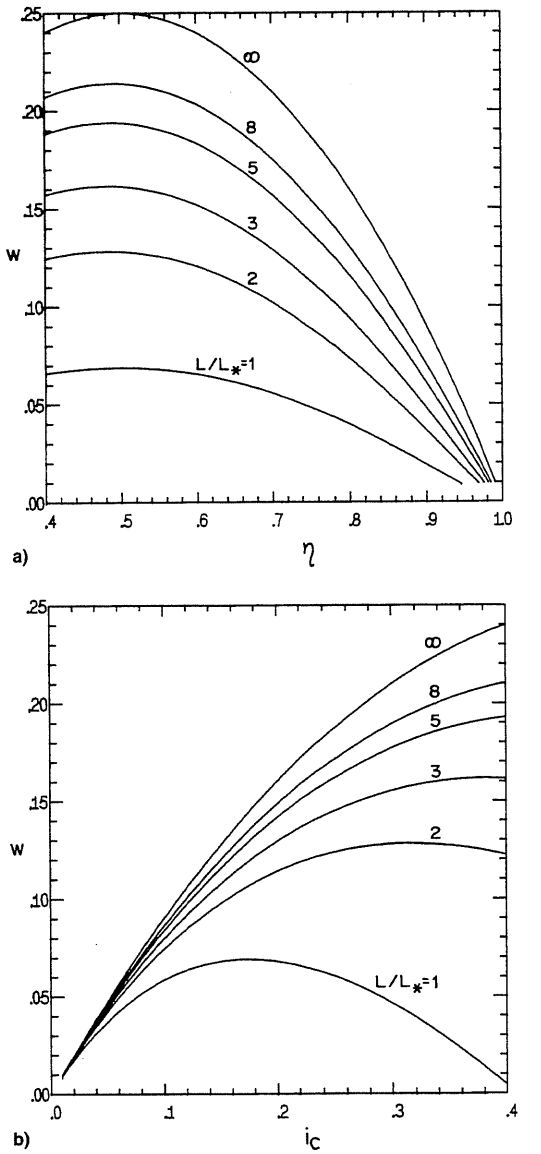

Fig. 3 Partially bare generator tether: dimensionless useful power w vs a) efficiency η, and b) fraction i_C of the short circuit current, for several values of the length parameter L/L_*. The line $L/L_* = \infty$ corresponds to the ideal tether limit.

Equations (9), (14), (16), and (19–21) yield

$$\eta = (1 - i_C)\left[1 + \frac{\xi_B(i_C) - \varphi_A(i_C)}{i_C\xi_B(i_C)}\frac{L_B}{L - L_B}\right]^{-1} \qquad (22)$$

$$w = i_C(1 - i_C)(1 - L_B/L), \qquad L_B/L = \xi_B(i_C)L_*/L \qquad (23)$$

Instead of the detailed characteristic $\Delta V_A(i_CJ_*A_t; n_\infty, T_\infty, B, \ldots)$ required in Eqs. (10) and (11), the new Eqs. (22) and (23) just add n_∞, appearing in Eq. (6) for L_*, to the input data E_m, ρ, J_*. As was the case for the standard tether, one may prove that $w(i_C, L_*/L)$ presents a maximum, for given L_*/L, at certain $i_C < \frac{1}{2}$, the best i_C range being centered at, say, 0.15. Figures 3a and 3b show $w(\eta, L_*/L)$ and $w(i_C, L_*/L)$. Also shown are ideal results $w = \eta(1 - \eta) = i_C(1 - i_C)$. They are recovered from Eqs. (22) and (23) in the limit $L_*/L \to 0$; as in the standard case, the efficiency is higher at fixed W_g and W_g/M (fixed A_tL and w), the higher L and the lower A_t (lower L_*). The approximation

$$(\xi_B - \varphi_A)/i_C\xi_B = \tfrac{3}{5} \qquad i_C < 0.4 \qquad (24)$$

is valid to within 1%; this considerably simplifies Eq. (22).

Consider standard and bare tethers with common values of L, W_g, and W_g/M, i.e., same w, A_t, and L. By also requiring a common efficiency in Eqs. (10) and (11), and (22) and (23), we determine the equivalent characteristic $\Delta V_A^s(I_C^s)$ of the bare tether; superscript s refers to values in the standard one, if different. Figure 4 shows $i_C^s \equiv I_C^s/J_* A_t$ vs $\varphi_A^s \equiv \Delta V_A^s/E_m L_*$ and L_*/L. The standard cable will be more efficient whenever its contactor operates at a point above the curve $i_C^s(\varphi_A^s)$ corresponding to some specific L_*/L. Clearly, the longer the cable, the more attractive is a bare tether, although, if long enough, both tethers approach the ideal behavior. For i_C^s (and i_C) small, we find

$$\varphi_A^s \simeq \tfrac{3}{5}(2i_C^s)^{2/3}[1 + (2L_*/3L)(2i_C^s)^{2/3} - (i_C^s/24) + \cdots]$$

For purposes of comparison we set the bracket equal to unity, the error being typically 10%, to get

$$\left[\frac{32\pi^2\varepsilon_0^2 e}{m_e (I_C^s)^2}\right]^{1/3} \Delta V_A^s \simeq \left(\frac{d_*}{d}\right)^{2/3} \tag{25}$$

here $d_* \equiv (\frac{3}{5})^{3/2} \times 6\pi\varepsilon_0 E_m/en_\infty$, or d_* (mm) $\simeq 0.96 \times 10^{11}$ m^{-3}/n_∞ at $E_m = 200$ V/km. For the passive spherical anode of Sec. II, use of $A_{\text{eff}} = I_C/J_\infty$ in Eq. (2), which ignored magnetic effects, yields Eq. (25) with F instead of $(d_*/d)^{2/3}$. A large area gain implies a large value of F. Since we usually have d_*/d small, the impedance of the sphere is substantially higher. The bare tether appears as an effective passive anode which, in addition, is unaffected by the magnetic field.

Consider now the condition for a tether to be near ideal (L_*/L small). There is no thermal obstacle to choosing a cable with small cross section. Assume the cable temperature T_t governed by a local balance of Ohmic heating, $I_C^2/\sigma A_t$, and radiation loss, $\pi d\varepsilon\sigma_B(T_t^4 - T_{\text{bk}}^4)$, with a background temperature $T_{\text{bk}} \sim 250$ K. This yields a value

$$T_t = T_{\text{bk}}[1 + (J_* E_m i_C^2 A_t^{1/2}/2\pi^{1/2}\varepsilon\sigma_B T_{\text{bk}}^4)]^{1/4}$$

which, at given i_C, is a weakly decreasing function of A_t [R is taken in Eq. (12) accordingly to maintain the appropriate current]. Length limitations arising from material strength (the maximum stress in the cable increases as L^2) or possible collisions with orbital debris (the frontal area increases as $L^{1/2}$ for given volume) would appear to allow values $L \sim 100$ km.[1] For a standard tether, the most stringent limitation on length would arise from the high-voltage insulation; a maximum voltage around 5 kV has been suggested.[1] The same would apply to a partially bare tether.

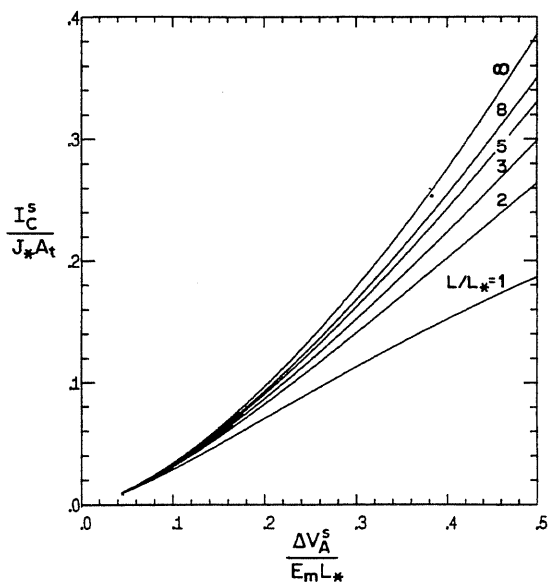

Fig. 4 Partially bare generator tether: equivalent contactor characteristic for different values of L/L_*.

This will limit somehow the power available at the load. To determine a bound on W_g, we use Eq. (12), as well as expressions Eqs. (6) and (21) for L_* and L_B. For aluminum, $E_m = 200$ V/km, and a maximum insulated length $L - L_B = 25$ km (peak bias 5 kV), we find

$$W_g^{\max}\ (\text{kW}) \simeq \frac{459(L_B/L)^3}{(1 - L_B/L)^4}\left(\frac{n_\infty}{10^{11}\ \text{m}^{-3}}\right)^2 \frac{w}{\xi_B^3}$$

A low value of L_B/L, though convenient in Eqs. (22) and (23), would make $W_g^{\max}$ too small. A compromise choice could be $L_B/L = \frac{1}{5}$. Then we have $w = \frac{4}{5} i_C(1 - i_C)$, $\eta = \frac{20}{23}(1 - i_C)$: at $w = 0.10$, the efficiency is $\eta \simeq 0.74$ ($\xi_B \simeq 0.46$). Also, we obtain $W_g^{\max} \simeq 10$ kW at night, $W_g^{\max} \simeq 1$ MW by day.

C. Fully Bare Tether

The above limitations on length and power disappear if the tether goes uninsulated over its entire length. The analysis of the segment AB in Fig. 1 may be taken from Sec. III.B; however, only the relation [Eq. (20)] between $\xi_B \equiv L_B/L_*$ and $\varphi_A \equiv \Delta V_A/E_m L_*$ is needed. The current here changes from a value I_B at point B to a value I_C through the load, at end C of the cable [we would write i_B, instead of i_C, in Eqs. (19) and (21)]. Along the ion-collecting segment BC we have

$$\frac{dI}{dy} = -en_\infty d(-2e\Delta V/m_i)^{1/2}, \qquad \Delta V < 0 \tag{26}$$

Equations (15) and (26) read, in dimensionless form

$$\frac{di}{d\xi} = -\frac{3}{4}\epsilon\psi^{1/2}, \qquad \frac{d\psi}{d\xi} = 1 - i$$

where we defined $\psi \equiv -\Delta V/E_m L_*$ and $\epsilon \equiv (m_e/m_i)^{1/2}$. Using Eq. (20), and boundary conditions $i = i_B$, $\psi = 0$ at $\xi = \xi_B$, and $i = i_C$, $\psi = RI_C/E_m L_* \equiv \psi_C$ at $\xi = L/L_*$, we obtain

$$2i_C - i_C^2 = \varphi_A^{3/2} - \epsilon\psi_C^{3/2} \tag{27}$$

$$\frac{L}{L_*} = \int_0^{\varphi_A} \frac{d\varphi}{(1 + \varphi^{3/2} - \varphi_A^{3/2})^{1/2}} + \int_0^{\psi_C} \frac{d\psi}{(1 + \epsilon\psi^{3/2} - \varphi_A^{3/2})^{1/2}} \tag{28}$$

The mechanical power is now

$$W_m = \int_0^L E_m I(y)\, dy = J_* A_t(E_m L - RI_C - \Delta V_A)$$

where we again write $RI_C = E_m L_* \psi_C$. Finally we arrive at

$$\eta = i_C\psi_C[(L/L_*) - \psi_C - \varphi_A]^{-1} \tag{29}$$

$$w = i_C\psi_C L_*/L \tag{30}$$

Figures 5a and 5b show $w(\eta, L_*/L)$ and $w(i_C, L_*/L)$, from Eqs. (27–30), for $\epsilon = \frac{1}{172}$. As w decreases with L_*/L fixed, η exhibits a relative maximum. Furthermore, taking the limit $L_*/L \to 0$ does not recover the ideal laws, $w(\text{ideal}) = \eta(1 - \eta) = i_C(1 - i_C)$, also shown in the figures. As advanced in Sec. II, this is a consequence of the decrease in current through the load, caused by substantial ion collection. The envelope of the family $w(\eta, L_*/L)$, L_*/L parameter, gives an upper bound $w_M(\eta)$, also shown in Fig. 5a, which corresponds to optimal conditions. For $\eta = 0.75$ we find $w_M \simeq 0.09$ or, using

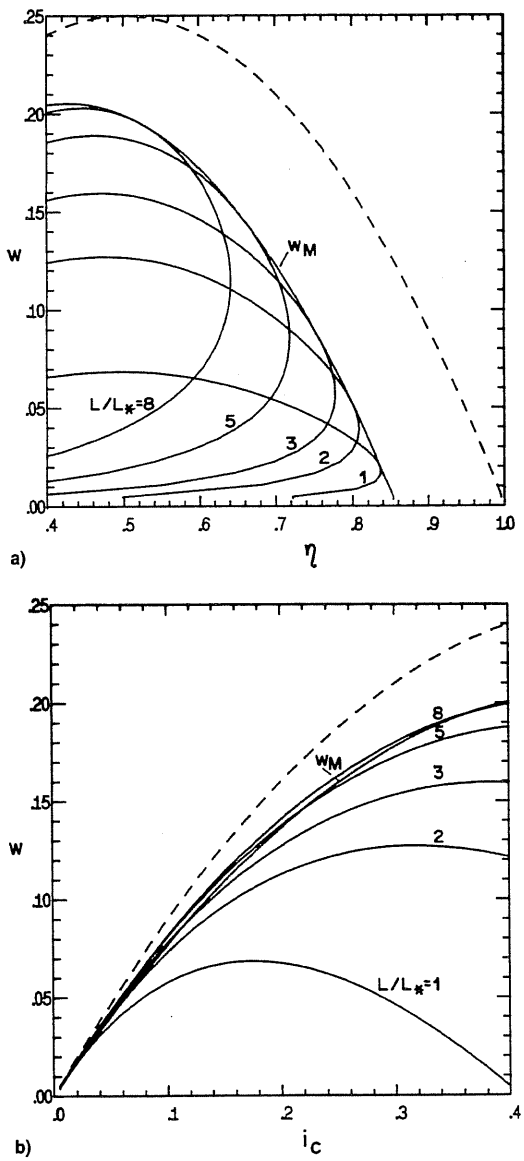

Fig. 5 Fully bare generator tether: w vs a) η, and b) i_C, for different values of L/L_* (solid lines). The dash-and-dot lines, $w_M(\eta)$ and $w_M(i_C)$, correspond to the envelope of the family $w(\eta, L/L_*)$ and represent optimal values. The ideal tether behavior (dashed line) is included for comparison.

Eq. (12), 21 kg of cable mass per kW of useful power. (Note that contrary to a standard tether, our fully bare generator does not require the additional dead weight of insulating material and an active anode.) Figure 5b exhibits the relation $i_C(w_M)$. Figure 6 presents L/L_*, L_B/L, and $(I_B - I_C)/I_B$ vs w_M.

One can now determine the geometry of the optimal tether for given power and ambient conditions. From Eqs. (6) and (12) for aluminum and $E_m = 200$ V/km, we can write

$$d\ (\text{mm}) \simeq 0.41 \left(\frac{W_g}{1\ \text{kW}}\right)^{3/8} \left(\frac{n_\infty}{10^{11}\ \text{m}^{-3}}\right)^{1/4} \frac{(L_*/L)^{3/8}}{w_M^{3/8}} \qquad (31)$$

At $\eta = 0.75$ ($w_M \simeq 0.09$) we obtain, from Fig. 6, $L/L_* \simeq 2.9$. For night densities then, d varies between 0.68–3.8 mm for W_g ranging from 1 to 100 kW; day values are increased by a factor $10^{1/4} \simeq 1.8$. For the length we find

$$L\ (\text{km}) \simeq 5.4 \left(\frac{W_g}{1\ \text{kW}}\right)^{1/4} \left(\frac{10^{11}\ \text{m}^{-3}}{n_\infty}\right)^{1/2} \frac{(L/L_*)^{3/4}}{w_M^{1/4}} \qquad (32)$$

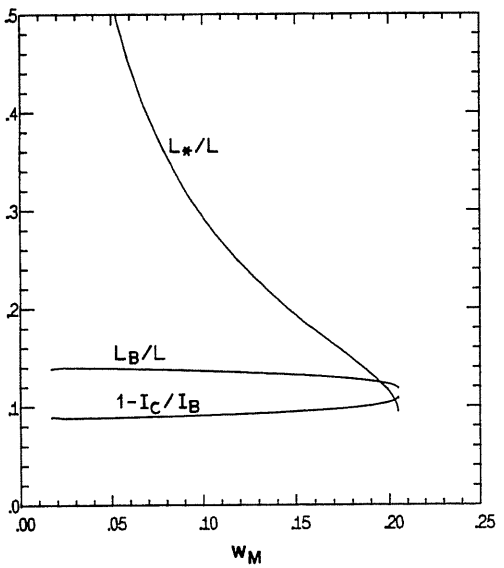

Fig. 6 Fully bare generator tether: length parameter L/L_*, anodic fraction of the tether L_B/L, and fractional ion-current loss $(I_B - I_C)/I_B$ for optimal values.

Note the weak dependence on power. At $\eta = 0.75$, for the night, L varies from 21.9 to 69.3 km in the 1–100 kW range; day lengths are smaller in the factor $10^{1/2} \simeq 3.2$. Diameter and length scale with inducting field and material conductivity as $E_m^{-7/8}\sigma^{-5/8}$ and $(\sigma/E_m)^{1/4}$, respectively.

Since the length L_B in Fig. 1 changes with ionospheric conditions, a partially bare tether could attract ions over some bare segment around point B; O^+ ion impacts, however, would produce no surface effects because such segment would be short and biased at low potentials. On the other hand, a fully bare tether would be highly negative over most of its length. We find that effects of the accelerated ions on the conductive surface are, nonetheless, weak. Secondary electron emission could affect results by 1% at most. Note first, that the ion current is itself small, $(I_B - I_C)/I_B \simeq \text{const} \simeq 0.09$ (Fig. 6). Secondly, the yield of secondary electrons per ion should be similarly small. For instance, the yield for bombardment of extremely clean aluminum by keV energy protons (oxygen and hydrogen having the same first ionization potentials) lies in the 0.1–0.2 range.[10] Furthermore, the formation of a protective oxide layer in the surface of the cable along segment BC would reduce both the ion current and its yield of secondary electrons.[11]

Concerning sputtering, note that this is a very slow process in ionospheric conditions because of the extremely low density of the ambient plasma. From Eq. (26) the ion current density at a point in segment BC, with local bias ΔV, is $en_\infty(2e\Delta V/\pi^2 m_i)^{1/2}$. For O^+ ions, a mean bias $\Delta V = 2$ kV, and a daytime density $n_\infty = 10^6$ cm^{-3}, we get 0.79×10^{-6} A/cm^2 or 4.93×10^{12} ions/cm^2 s. Since there are 6.02×10^{22} Al atoms/cm^3, a sputtering yield of one atom per ion gives an erosion speed of 0.013 mm/yr (we assumed that half the time the density takes night values, $n_\infty << 10^6$ cm^{-3}). For a cable with an initial radius of 2 mm, that erosion amounts to 6.5% in 10 yr. A yield of one atom per ion is an estimate consistent with experimental results on sputtering of Al by Hg^+,[12] and inert gas ions,[13] although again an oxyde layer would actually reduce the sputtering.[1] Note that the ambient plasma has virtually no damaging multiply-charged ions.

IV. Thruster Mode

A. Standard Tether

The circuit equation for a standard thruster is

$$\mathcal{E} = E_m L + (L/\sigma A_t) I_C + \Delta V_A \qquad (33)$$

Given E_m, J_*, and the anode characteristic $\Delta V_A(I_C)$, Eq. (33) yields I_C for selected values of L, A_t, and the supply electromotive force $\mathcal{E}$; we shall assume $\mathcal{E} > E_m L$ so as to have positive I_C and ΔV_A in Eq. (33). The useful mechanical power W_m ($\tilde{f} \cdot \tilde{v}_{orb}$, where $\tilde{f}$ is the thrust) is $W_m = E_m L I_C$. We then define both a thruster efficiency $\eta \equiv W_m/\mathcal{E}I_C$ and a dimensionless useful power per unit mass $w \equiv \rho W_m/E_m J_* M$, and find

$$\eta = [1 + i_C + \Delta V_A(i_C J_* A_t)/E_m L]^{-1}, \qquad w = i_C \tag{34}$$

also

$$W_m = J_* E_m A_t L w, \qquad W_m/M = J_* E_m w/\rho \tag{35}$$

$$\mathcal{E} = E_m L w/i_C \eta, \qquad I_C = J_* A_t i_C \tag{36}$$

For selected values of A_t, L, and say, w, we can determine all other quantities of interest. For ΔV_A negligible (ideal thruster) we have $\eta = (1 + w)^{-1}$; best ranges would be centered around $w = i_C = 0.25$, $\eta = 0.8$. For a real tether with given values of W_m and W_m/M, long, thin cables are favored, as in the case of generators, because $\Delta V_A/E_m L$ is reduced on both counts; insulation problems would limit the length L. The dimensionless current i_C should be somewhat lowered to make w and η share the negative effects of the anodic impedance.

B. Bare Tether

As will be seen below, a fully uninsulated tether working as a thruster is inefficient. Consequently, we leave bare only an anodic segment AB in Fig. 2. The circuit equation may now be written as

$$\mathcal{E} = \Delta V_B + (E_m + I_C/\sigma A_t)(L - L_B)$$

where L_B is given, and ΔV_B is the highest anodic bias at the beginning of the insulated part. Since the thruster is downward deployed we have $V_p = -E_m y$ (Fig. 2), and the equation governing the bias voltage is

$$\frac{d\Delta V}{dy} = E_m + I/\sigma A_t \tag{37}$$

Using Eq. (37) we find

$$W_m = \int_0^L E_m I(y)\, dy = E_m I_C(L - L_B) + J_* A_t(\Delta V_B - \Delta V_A - E_m L_B)$$

Equations for both ΔV_A and ΔV_B are now needed.

We shall consider $\Delta V_A \geq 0$ (an ion-attracting segment at end A of the wire would have a negative, though insignificant, effect on the circuit; it would just be dead weight). $\mathcal{E}$ then must exceed some value if A_t, L, and L_B are given. Introducing the dimensionless variables ξ, φ, i of Sec. III, we proceed similarly. Equations (3) and (37) become $di/d\xi = \frac{3}{4}\varphi^{1/2}$, $d\varphi/d\xi = 1 + i$, from which, using boundary conditions $\varphi = \varphi_A$, $i = 0$ at $\xi = 0$ and $\varphi = \varphi_B$, $i = i_C$ at $\xi = \xi_B$, we obtain

$$\varphi_B^{3/2} - \varphi_A^{3/2} = 2i_C + i_C^2 \tag{38}$$

$$\xi_B = \int_{\varphi_A}^{\varphi_B} d\varphi(1 + \varphi^{3/2} - \varphi_A^{3/2})^{-1/2} \tag{39}$$

with

$$\Delta V_A = E_m L_* \varphi_A, \quad \Delta V_B = E_m L_* \varphi_B, \quad L_B = L_* \xi_B$$

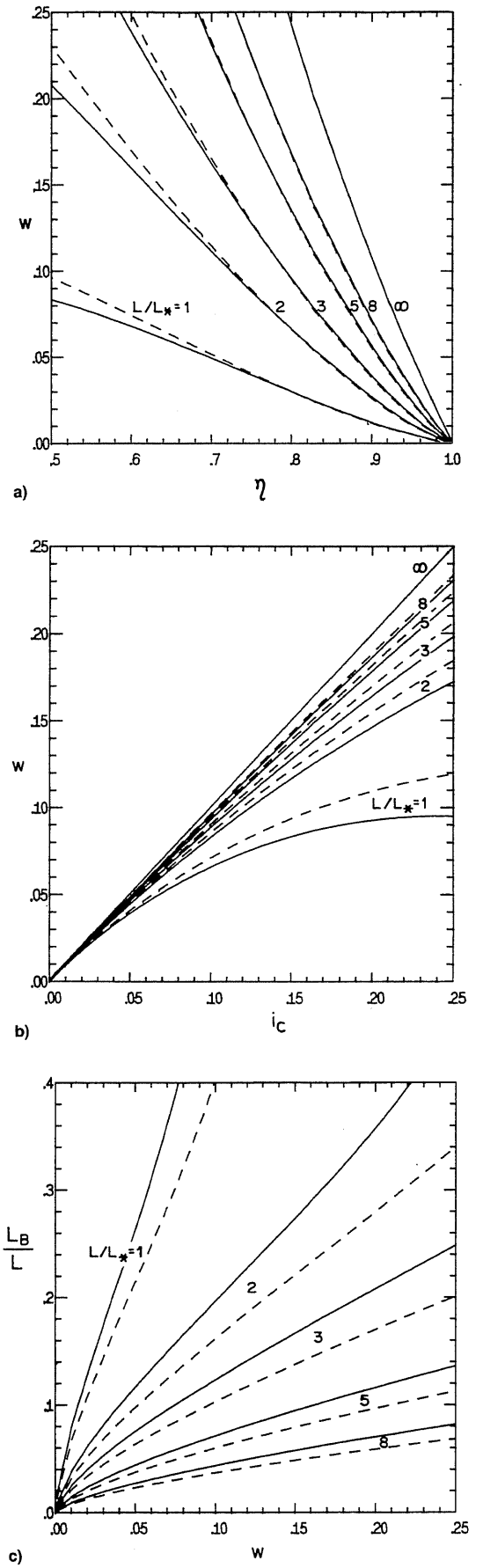

Fig. 7 Partially bare thruster tether: a) dimensionless useful power w vs efficiency η, b) w vs i_C, and c) L_B/L vs w, for different values of L/L_* and $x \equiv \Delta V_A/\Delta V_B$ equal to 0 (solid lines) and 0.2 (dashed lines).

We then find

$$\eta = \left(1 + \frac{L_B}{L - L_B}\frac{\varphi_B - \varphi_A - \xi_B}{i_C \xi_B}\right) \Bigg/ \left(1 + i_C + \frac{L_B}{L - L_B}\frac{\varphi_B}{\xi_B}\right) \tag{40}$$

$$w = i_C\left[1 - \frac{L_B}{L}\left(1 - \frac{\varphi_B - \varphi_A - \xi_B}{i_C \xi_B}\right)\right] \tag{41}$$

Use of Eqs. (38) and (39) in Eqs. (40) and (41), determines w and η as functions of i_C, for given L_B/L and L_B/L_*; alternatively, one can give L_*/L and $x \equiv \varphi_A/\varphi_B$.

For $L_B = L$, the above equations yield results for a fully bare thruster. At small i_C we obtain, in particular

$$\eta = \tfrac{2}{5} - \tfrac{3}{5}[x^{3/2}(1 - x)/(1 - x^{3/2})]$$

The maximum efficiency, 0.4, which occurs at $x = 0$, is too low.

As in the case of the generator, we can determine the equivalent characteristic $\Delta V_A^s(I_C^s)$ of the bare thruster, by comparing Eq. (34) and Eqs. (38–41) for common values of w, A_t, L, and efficiency. For small i_C, we find

$$(\Delta V_A^s/E_m L_*) \simeq \tfrac{3}{5}(2i_C^s)^{2/3}[(1 - x^{5/2})/(1 - x^{3/2})^{5/3}]$$

Again, the bare tether, as an anodic contactor, works most efficiently at $x = 0$, when Eq. (25) is recovered.

Figures 7a–c show $w(\eta)$, $w(i_C)$, and the ratio L_B/L vs w, for several values of L_*/L and x. For given L_*/L and high efficiency, w is maximum at $x = 0$, but as η decreases the maximum moves to some positive $x(\eta)$. For the moderately high efficiencies of interest, however, there is no practical advantage to considering nonzero values for x. For $x = 0$ and i_C small, Eqs. (39–41) become

$$\xi_B \simeq \varphi_B\left(1 + \frac{3}{5}i_C\right)^{-1}, \qquad w \simeq i_C\left(1 - \frac{3}{5}\frac{L_B}{L}\right) \tag{42}$$

$$\eta \simeq \left[1 + \frac{2}{5}\frac{L_B}{L - L_B}\right] \Bigg/ \left[1 + i_C + \frac{L_B}{L - L_B}\left(1 + \frac{2}{5}i_C\right)\right] \tag{43}$$

which are valid to within 1% for $i_C < 0.27$.

Taking the limit $L_*/L \to 0$ in Figs. 7a and 7b recovers ideal laws $w = (1 - \eta)/\eta = i_C$, also shown in the figures. High-voltage insulation problems, however, again limit the length L. Now the peak bias is close to $E_m L$; if this bias is not to exceed 5 kV, and for $E_m = 200$ V/km, we must have $L \leq 25$ km. From Eqs. (6) and (12), and $L = 25$ km, we then obtain, for aluminum, a maximum power

$$W_m^{\max}\ (\text{kW}) \simeq 459(L_B/L)(w/\xi_B^3)(n_\infty/10^{11}\ \text{m}^{-3})^2$$

A low ratio L_B/L, although convenient in Eqs. (42) and (43), would produce too small a value $W_m^{\max}$. A compromise choice, $L_B/L = \frac{1}{4}$, gives $\eta = 17(20 + 17i_C)^{-1}$, $w = 17i_C/20$; at $i_C = 0.14$, we find $\eta \simeq 0.76$, $w \simeq 0.12$ ($\xi_B \simeq 0.42$). For the maximum power we obtain $W_m^{\max} \simeq 12$ kW at night, and $W_m^{\max} \simeq 1.2$ MW by day.

V. Conclusions

A simple approach to the problem of electron collection by high-power electrodynamic tethers has been presented in detail. The scheme requires no specialized hardware, and relies solely on passive collection by a multikilometer long, uninsulated segment of the cable. With a radius less than both Debye length and thermal gyroradius, effects due to electric shielding or magnetic channeling are avoided, electrons being collected in the OML regime. There are no major uncertainties in the theory of operation, which we have developed for both thrusting and generation in limited density ranges; simple formulas and charts are presented for quick reference. Altogether the fact that a complex contactor at the end of a wire tens of kilometers long is not relied upon, and the simplicity of our device, make it ideal for (early) implementation of electrodynamic tether systems. Since the current is kept at a small fraction of its short-circuit value, wire deflection caused by the magnetic force is small.

Efficient generation of current (and simultaneous electrodynamic braking) may be achieved with a fully bare cable; the elimination of insulation problems allows using thinner, longer cables that provide unlimited power. More efficient generation and propulsion are achieved by using partially bare tethers; maximum power is about 10 kW at night, and 1 MW by day. Larger powers might be accommodated by wrapping a metallized jacket on a nonconductive, light cable in the uninsulated segment; the use of an auxiliary standard anode to collect an additional fraction of the current has been just studied.[14]

Acknowledgments

This work was supported by Comision Interministerial de Ciencia y Tecnología of Spain (Project ESP89-0170). The stay of E. Ahedo at M.I.T. was supported by a Fulbright Scholarship from Spain. We acknowledge helpful criticism by the referees.

References

[1]Martínez-Sánchez, M., and Hastings, D. E., "A Systems Study of a 100 kW Tether," *Journal of the Astronautical Sciences*, Vol. 35, No. 1, 1987, pp. 75–96.

[2]Wilbur, P., and Laupa, T., "Plasma Contactor Design for Electrodynamic Tether Applications," *Advances in Space Research*, Vol. 8, No. 1, 1988, pp. 221–224.

[3]Gerver, M. J., Hastings, D. E., and Oberhardt, M., "Theory of Plasma Contactors in Ground-Base Experiments and Low Earth Orbit," *Journal of Spacecraft and Rockets*, Vol. 27, No. 4, 1990, pp. 391–402.

[4]Lam, S., "Unified Theory for the Langmuir Probe in a Collisionless Plasma," *Physics of Fluids*, Vol. 8, No. 1, 1965, pp. 73–87.

[5]Ahedo, E., Martínez-Sánchez, M., and Sanmartín, J., "Current Collection by an Active Spherical Electrode in an Unmagnetized Plasma," *Physics of Fluids B*, Vol. 4, No. 12, pp. 3847–3855.

[6]Laframboise, J. G., "Theory of Spherical and Cylindrical Langmuir Probes in a Collisionless, Maxwellian Plasma at Rest," Univ. of Toronto, Inst. for Aerospace Studies Rept. 100, Toronto, Canada, 1966.

[7]Rubinstein, J., and Laframboise, J. G., "Upper-Bound Current to a Cylindrical Probe in a Collisionless Magnetoplasma," *Physics of Fluids*, Vol. 21, No. 9, 1978, pp. 1655, 1656; "Theory of a Spherical Probe in a Collisionless Magnetoplasma," *Physics of Fluids*, Vol. 25, No. 7, 1982, pp. 1174–1182.

[8]Chung, P. M., Talbot, L., and Touryan, K. J., *Electric Probes in Stationary and Flowing Plasmas*, Vol. 11, Springer-Verlag, New York, 1975.

[9]Hastings, D. E., and Wang, J., "The Radiation Impedance of an Electrodynamic Tether with End Connectors," *Geophysics Research Letters*, Vol. 14, No. 5, 1987, pp. 519–522.

[10]Baragiola, R. A., Alonso, E. V., and Oliva Florio, A., "Electron Emission from Clean Metal Surfaces Induced by Low-Energy Light Ions," *Physical Review B*, Vol. 19, No. 1, 1979, pp. 121–129.

[11]Brown, S. C., *Basic Data of Plasma Physics*, Wiley, New York, 1959; see also Kaminsky, M., *Atomic and Ionic Impact Phenomena on Metal Surfaces*, Academic Press, New York, 1965.

[12]Schott, L., "Electrical Probes," *Plasma Diagnostics*, edited by W. Lochte-Holgreven, North-Holland, Amsterdam, 1968, p. 703.

[13]Sigmund, P., "Theory of Sputtering. I. Sputtering Yield of Amorphous and Polycrystalline Targets," *Physical Review*, Vol. 184, No. 2, 1969, pp. 383–416.

[14]Samanta Roy, R. I., Hastings, D. E., and Ahedo, E., "A Systems Analysis of Electrodynamic Tethers," *Journal of Spacecraft and Rockets*, Vol. 29, No. 3, 1992, pp. 415–424.

Given E_m, J_*, and the anode characteristic $\Delta V_A(I_C)$, Eq. (33) yields I_C for selected values of L, A_t, and the supply electromotive force $\mathscr{E}$; we shall assume $\mathscr{E} > E_m L$ so as to have positive I_C and ΔV_A in Eq. (33). The useful mechanical power W_m ($\underset{\sim}{f}\cdot\underset{\sim}{v}_{orb}$, where $\underset{\sim}{f}$ is the thrust) is $W_m = E_m L I_C$. We then define both a thruster efficiency $\eta \equiv W_m/\mathscr{E}I_C$ and a dimensionless useful power per unit mass $w \equiv \rho W_m/E_m J_* M$, and find

$$\eta = [1 + i_C + \Delta V_A(i_C J_* A_t)/E_m L]^{-1}, \qquad w = i_C \tag{34}$$

also

$$W_m = J_* E_m A_t L w, \qquad W_m/M = J_* E_m w/\rho \tag{35}$$

$$\mathscr{E} = E_m L w/i_C \eta, \qquad I_C = J_* A_t i_C \tag{36}$$

For selected values of A_t, L, and say, w, we can determine all other quantities of interest. For ΔV_A negligible (ideal thruster) we have $\eta = (1 + w)^{-1}$; best ranges would be centered around $w = i_C = 0.25$, $\eta = 0.8$. For a real tether with given values of W_m and W_m/M, long, thin cables are favored, as in the case of generators, because $\Delta V_A/E_m L$ is reduced on both counts; insulation problems would limit the length L. The dimensionless current i_C should be somewhat lowered to make w and η share the negative effects of the anodic impedance.

B. Bare Tether

As will be seen below, a fully uninsulated tether working as a thruster is inefficient. Consequently, we leave bare only an anodic segment AB in Fig. 2. The circuit equation may now be written as

$$\mathscr{E} = \Delta V_B + (E_m + I_C/\sigma A_t)(L - L_B)$$

where L_B is given, and ΔV_B is the highest anodic bias at the beginning of the insulated part. Since the thruster is downward deployed we have $V_p = -E_m y$ (Fig. 2), and the equation governing the bias voltage is

$$\frac{d\Delta V}{dy} = E_m + I/\sigma A_t \tag{37}$$

Using Eq. (37) we find

$$W_m = \int_0^L E_m I(y)\, dy = E_m I_C(L - L_B)$$

$$+ J_* A_t(\Delta V_B - \Delta V_A - E_m L_B)$$

Equations for both ΔV_A and ΔV_B are now needed.

We shall consider $\Delta V_A \geq 0$ (an ion-attracting segment at end A of the wire would have a negative, though insignificant, effect on the circuit; it would just be dead weight). $\mathscr{E}$ then must exceed some value if A_t, L, and L_B are given. Introducing the dimensionless variables ξ, φ, i of Sec. III, we proceed similarly. Equations (3) and (37) become $di/d\xi = \frac{3}{4}\varphi^{1/2}$, $d\varphi/d\xi = 1 + i$, from which, using boundary conditions $\varphi = \varphi_A$, $i = 0$ at $\xi = 0$ and $\varphi = \varphi_B$, $i = i_C$ at $\xi = \xi_B$, we obtain

$$\varphi_B^{3/2} - \varphi_A^{3/2} = 2i_C + i_C^2 \tag{38}$$

$$\xi_B = \int_{\varphi_A}^{\varphi_B} d\varphi(1 + \varphi^{3/2} - \varphi_A^{3/2})^{-1/2} \tag{39}$$

with

$$\Delta V_A = E_m L_* \varphi_A, \quad \Delta V_B = E_m L_* \varphi_B, \quad L_B = L_* \xi_B$$

ERRATUM: These are correct plots for Fig. 7. The original ones were based on $w = i_C(1 - \xi_B/\xi_C)$.

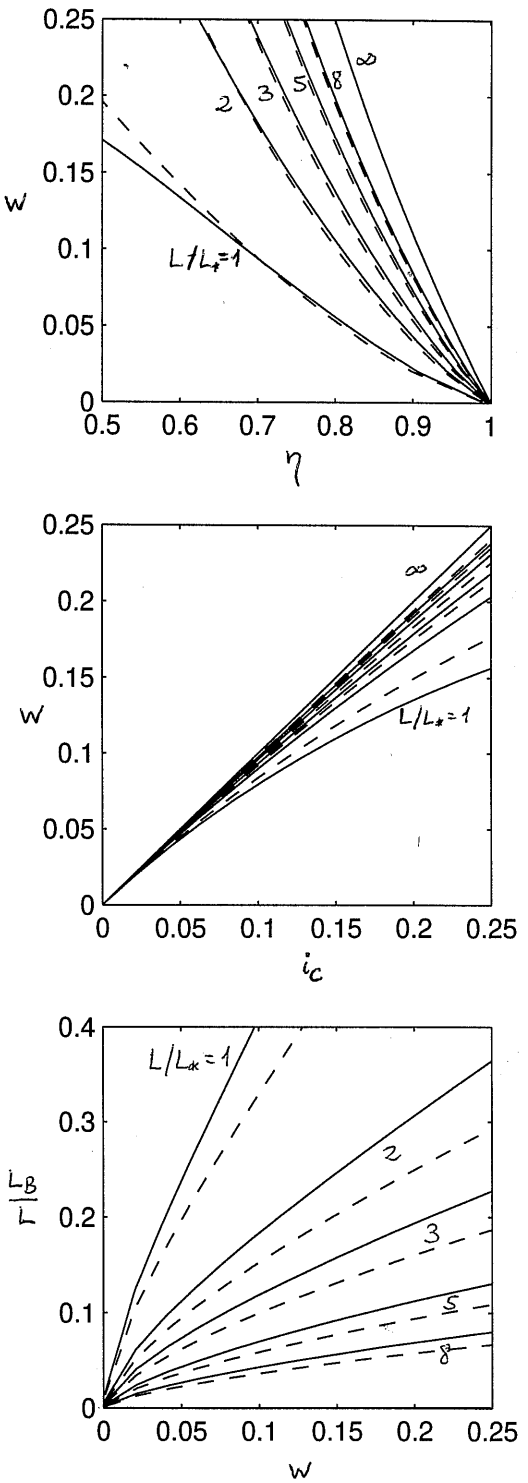

Fig. 7 Partially bare thruster tether: a) dimensionless useful power w vs efficiency η, b) w vs i_C, and c) L_B/L vs w, for different values of L/L_* and $x \equiv \Delta V_A/\Delta V_B$ equal to 0 (solid lines) and 0.2 (dashed lines).

View publication stats